



## Physical interactions in macroporous scaffolds based on poly( $\epsilon$ -caprolactone)/chitosan semi-interpenetrating polymer networks

Dunia M. García Cruz<sup>a</sup>, Daniela F. Coutinho<sup>b,c</sup>, João F. Mano<sup>b,c</sup>, José Luis Gómez Ribelles<sup>a,d,e</sup>, Manuel Salmerón Sánchez<sup>a,d,e,\*</sup>

<sup>a</sup>Center for Biomaterials and Tissue Engineering, Universidad Politécnica de Valencia, 46022 Valencia, Spain

<sup>b</sup>3B's Research Group – Biomaterials, Biodegradables and Biomimetics, Dept. of Polymer Engineering, University of Minho, Campus de Gualtar, 4710-057 Braga, Portugal

<sup>c</sup>IBB – Institute for Biotechnology and Bioengineering, Braga, Portugal

<sup>d</sup>Laboratorio de Biomateriales, Centro de Investigación Príncipe Felipe, Autopista del Saler 16, 46013 Valencia, Spain

<sup>e</sup>CIBER en Bioingeniería, Biomateriales y Nanomedicina, Valencia, Spain

### ARTICLE INFO

#### Article history:

Received 23 August 2008

Received in revised form

26 February 2009

Accepted 27 February 2009

Available online 11 March 2009

#### Keywords:

Biodegradable scaffolds

Chitosan

Poly( $\epsilon$ -caprolactone)

### ABSTRACT

Polycaprolactone (PCL) and chitosan (CHT) are immiscible polymers. However, biodegradable porous scaffolds of both polymers were obtained by combining different techniques based on the synthesis of semi-interpenetrating polymer networks (SemilPNs) and melt processing. SemilPNs were prepared through simultaneous precipitation of the polymer blend (PCL/CHT) and subsequent crosslinking of chitosan with tripolyphosphate (weight fractions of CHT up to 30 wt.%). High porosity PCL/CHT scaffolds with open pore structure and good interconnectivity were obtained. Mechanical properties, evaluated by dynamic-mechanical analysis, decrease as porosity increases. The physical interactions between functional groups of CHT and carbonyl groups of PCL were assessed by FTIR, the shifting of the main relaxation of PCL towards high temperatures as the fraction of CHT increases as well as the evolution of the thermal properties of the system.

© 2009 Elsevier Ltd. All rights reserved.

### 1. Introduction

Tissue engineering approach requires scaffolds to provide a short-term three-dimensional substrate to cell growth, adhesion and proliferation as well as enabling the transport of cell nutrients and wastes, and providing suitable mechanical properties after implantation. A variety of natural and synthetic polymeric materials are being tested as scaffolds for regenerative medicine and tissue repair. Synthetic polyesters like polycaprolactone (PCL) have become a versatile material in cardiovascular, bone, cartilage tissue engineering, pharmaceutical controlled release systems, and in biodegradable packaging [1–5]. PCL is thermoplastic aliphatic polyester which can be easily processed into complicated three-dimensional architectures using conventional technologies due to its low melting point, and low viscosity. Mechanical properties and degradation mechanism of PCL can be altered by chemical modification. Many efforts have been devoted to the exploration of the chemical modification of  $\epsilon$ -caprolactone to synthesize a monomer that can be

copolymerized with other hydrophilic comonomers [6]. On the other hand, blending techniques were widely used to modify physical and chemical properties of aliphatic polyesters. Blending polymeric materials like PCL with biodegradable natural biopolymers such as starch, cellulose, chitosan and chitin have been explored in the past [7–11]; the production of biodegradable polymers using these renewable resources is nowadays increasing [12]. For tissue engineering applications, it is expected that the homogeneous blending of a hydrophilic polymer with the hydrophobic PCL chains improves water diffusion to the proximities of PCL chains, thus accelerating their hydrolytic degradation. An increase of PCL wettability is also desired when three-dimensional scaffolds are prepared to make cell seeding and nutrients diffusion in cell culture easier. In this work, chitosan (CHT) was employed as the hydrophilic, biodegradable component. CHT is a polymer derived of the partial deacetylation of chitin, a natural polymer that has become an important material in several fields including medicine, chemical industry and tissue engineering, due to its easy processing into films and scaffolds [13].

PCL and CHT are immiscible [9,13]; thus their blends are difficult to achieve due to the lack of common solvents and the impossibility of melt processing of CHT. Even though several blending processes have been proposed in the literature, it is difficult to produce three-dimensional (3D) scaffolds out of these blends. Sarasam et al.

\* Corresponding author. Center for Biomaterials and Tissue Engineering, Universidad Politécnica de Valencia, 46022 Valencia, Spain. Tel.: +34 96 3877275; fax: +34 96 3877276.

E-mail address: [masalsan@fis.upv.es](mailto:masalsan@fis.upv.es) (M. Salmerón Sánchez).

corroborated this feature, demonstrating that stable scaffolds of PCL and CHT mixture could not be obtained using processing techniques like freeze extraction, freeze gelation and freeze drying [14].

In this study we propose to prepare porous materials from blends of PCL and CHT, through the creation of a semi-interpenetrating polymer network (semiIPN), as a novel method to obtain CHT/PCL biodegradable porous scaffolds. SemiIPN consists of two polymeric materials, one of them in the form of a polymer network and the other one, uncrosslinked, occupying the same volume. The network structure of the former entraps the linear chains of the second component hindering their diffusion and enabling the formation of a homogeneous dispersion of the two immiscible polymers that otherwise would phase separate with large phase domains and poor mechanical properties [15].

PCL/CHT semiIPN system was prepared through the physical crosslinking of chitosan with sodium tripolyphosphate (TPP) entrapping PCL chains. Afterwards, porous scaffolds were prepared by melt processing and leaching out techniques. Morphology and properties of the system obtained are investigated.

## 2. Experimental section

Chitosan (CHT) from crab shells (practical grade), with a degree of deacetylation of 85% and molecular weight of 155 kDa was purchased from Sigma–Aldrich. Poly( $\epsilon$ -caprolactone) (PCL) and poly(ethylene oxide) (PEO), with molecular weight 48 and 100 kDa respectively were supplied by Polyscience. All the other reagents are analytical grade and were used without further purification.

### 2.1. Preparation of PCL/CHT semiIPNs

Chitosan and poly( $\epsilon$ -caprolactone) were dissolved in aqueous solution of acetic acid (1% v/v) and glacial acetic acid respectively and then, both solutions were mixed in adequate proportions to obtain PCL/CHT semiIPNs containing 10, 20 and 30 wt.% of CHT, after precipitation, in excess 0.3% (w/v) sodium tripolyphosphate solution with vigorous stirring. Chitosan is polycationic when dissolved in acid and presents  $-\text{NH}_3^+$  sites. Sodium tripolyphosphate dissolved in water dissociates to give both hydroxyl and phosphoric ions. Since the crosslinking of chitosan would be dependant on the availability of the cationic sites and negatively charged species to form a physical network. In this sense, when a solution of both polymers is added to a sodium tripolyphosphate solution, crosslinking of chitosan makes possible the entrapping of PCL chains within the chitosan network (see Fig. 1). The semiIPNs obtained in form of white powder were then suspended in a 0.1 M sodium hydroxide solution, to neutralize and then washed with abundant distilled water to reach pH 7. Finally, the samples were dried in vacuum to constant weight.

### 2.2. Preparation of PCL/CHT porous scaffolds

PCL/CHT scaffolds with varying porosity were prepared from semiIPNs using 0 wt.% (without any porogen), 30 wt.%, 45 wt.% or 55 wt.% of PEO, as porogen. PCL/CHT semiIPNs with different compositions (10, 20 and 30 wt.% CHT) were carefully triturated into powders, and mixed with sieved PEO particles (size range: 106–150  $\mu\text{m}$ ) and each mixture was loaded into a circular mould (30 mm diameter and 1.5 mm thickness). Afterwards, the mould was placed in an oven at 90 °C for 1 h allowing both PCL and PEO to melt. Subsequent cooling of the mould gives rise to PCL and PEO crystallization which sinters semiIPN particles and porogen PEO particles producing co-continuous phases. Then, the PCL/CHT scaffolds were immersed in water for 3 days at room temperature in a shaking plate, in order to completely remove the porogen from

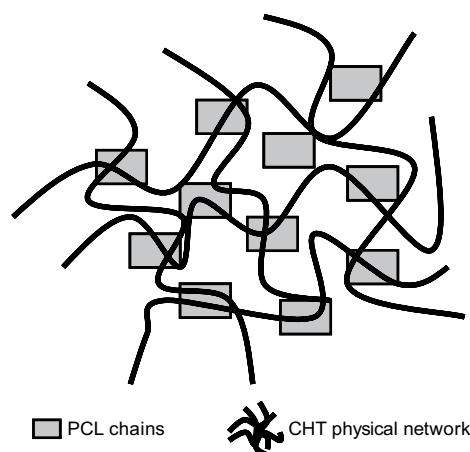


Fig. 1. Sketch of the spatial distribution in PCL/CHT semiIPNs. Physical crosslinking of CHT is achieved by sodium tripolyphosphate leaving PCL chains within the CHT network.

the scaffolds. Water was changed twice a day. Besides, films of neat PCL prepared by solvent casting technique and CHT networks crosslinked with sodium tripolyphosphate were used to compare with the obtained results for PCL/CHT semiIPNs.

### 2.3. Fourier transform infrared spectroscopy (FTIR)

FTIR spectra of semiIPNs were recorded on a Thermo Nicolet Nexus FTIR, controlled by OMNIC software, using the *Smart Diffuse Reflectance* method. The samples were used in powder and the reference was dried KBr. The spectra were obtained by accumulating 32 scans in the range 600–4000  $\text{cm}^{-1}$  with a resolution of 4  $\text{cm}^{-1}$ .

### 2.4. Swelling in simulated body fluid (SBF)

Swelling degree of the PCL/CHT scaffolds was gravimetrically measured in simulated body fluid (SBF, solution with an ion concentration nearly equal to that of human blood plasma and a pH of 7.4), prepared for this study according to the method described in Ref. [16]. Dry cylindrical samples, 5 mm diameter and approx. 1 mm thickness, were immersed in SBF at 37 °C. The weight of the samples was measured after different time periods up to 9 days, when equilibrium was reached. Before each weighting, the samples were removed from SBF and the excess of liquid on the surface was wiped off with a filter paper. Each reported value is the average of three replicate samples. The swelling degree is expressed as the amount of SBF per unit mass of dry polymer:

$$w = \frac{m_{\text{SBF}}}{m_{\text{drypolymer}}} \quad (1)$$

### 2.5. Density and porosity measurements

The PCL/CHT scaffolds were cut into a cylindrical piece (5 mm diameter and 1 mm thickness) and dried under vacuum for 24 h. The apparent density of PCL/CHT scaffolds ( $\rho_{\text{scaffold}}^*$ ) was calculated from the dried weight and volume of a scaffold as measured geometrically. The porosity ( $P$ ) of PCL/CHT scaffolds was determined to be,

$$P(\%) = \frac{(\rho_{\text{PCL/CHT}} - \rho_{\text{scaffold}}^*)}{\rho_{\text{PCL/CHT}}} \times 100 \quad (2)$$



Fig. 2. Photographs of neat chitosan (CHT), polycaprolactone (PCL) and PCL/CHT blends poured in a solution containing excess of sodium tripolyphosphate.

where,  $\rho_{\text{PCL/CHT}}$  was the density of PCL/CHT membrane (non-porous) semiIPNs with 10 wt.%, 20 wt.% and 30 wt.% of CHT as calculated by weighting in *n*-octane.

### 2.6. Scanning electron microscopy (SEM)

SEM analysis of the scaffolds was carried out in a scanning electron Jeol JSM-5410 microscope and performed on both longitudinal and transversal cross-sections (cryogenically fractured) of the samples. All specimens were coated with a conductive layer of sputtered gold. The micrographs were taken at an accelerating voltage of 15 kV in order to ensure a suitable image resolution.

### 2.7. Differential scanning calorimetry (DSC)

Differential scanning calorimetry (DSC) was performed in a Pyris 1 apparatus (PerkinElmer). Nitrogen gas was purged through the DSC cell with a flow rate of 20 ml/min. The temperature of the equipment was calibrated by using Indium and Zinc. The melting heat of Indium was used for calibrating the heat flow. After erasing the effects of any previous thermal history, by heating at 90 °C, the samples were subjected to a cooling scan down to –20 °C at 10 °C/min, followed by a heating scan from that temperature up to 90 °C at a rate of 10 °C/min. The characteristic transition temperatures have been calculated from the DSC curves.

### 2.8. Dynamic-mechanical analysis (DMA)

Dynamic-mechanical analysis was performed in a Seiko DMS210 apparatus at a frequency of 1 Hz in the tension mode (the static strain was automatically selected by the equipment so that pure tension is always applied). The stress–strain range was low enough so as to consider linear viscoelasticity to be valid. The temperature dependence of the storage modulus and loss angle was measured in the temperature range from –120 °C to 90 °C at a rate of 2 °C/min. The samples for these experiments were prismatic (ca. 20 × 5 × 1 mm<sup>3</sup>).

### 2.9. Thermogravimetric analysis (TGA)

Thermal stability measurements were performed using a TA-Instrument Model SDT-Q600 system. TGA test was performed in alumina crucibles where samples (5–10 mg weight) were placed on the balance and the temperature rose from 30 to 750 °C at a heating rate of 10 °C/min. The mass of the sample pan was continuously monitored as a function of temperature. TGA experiment was carried out in nitrogen environment using a flow rate 50 ml/min in order to avoid termooxidative degradation.

## 3. Results

### 3.1. PCL and CHT miscibility and their interactions in the semiIPNs

One of the first questions which arises when characterizing the semiIPNs obtained is whether the interpenetration between PCL chains and CHT network yields a homogeneous blend in which PCL and CHT chains are mixed at molecular level or phase separation takes place in some extent as it happens in a PCL/CHT polymer blends [9,10]. To answer this question, DSC, DMA, FTIR, and TGA measurements were performed on the semiIPN samples prepared without any porogen.

When neat chitosan, polycaprolactone and PCL/chitosan blends were poured in sodium tripolyphosphate solution, the neat chitosan became a physical network as it is evident from Fig. 2 that shows a gel with (transparent) water around. However, PCL precipitates in contact with water and a turbid solution appears. Crosslinking CHT in the presence of PCL allows one to entrap PCL chains within the CHT semiIPN for 20 and 30 wt.% of CHT (transparent solutions in Fig. 2). Nevertheless, only a part of PCL chains can be retained for the 10 wt.% system, giving rise to a system that consists of PLC chains entrapped within the CHT network (the gel) and non-incorporated PCL that is the reason for the turbid appearance of the solution (Fig. 2).

The influence of the amount of CHT on the PCL/CHT semiIPN on the thermal properties of PCL was studied by DSC. The crystallization thermograms, recorded on cooling at 10 °C/min are shown in Fig. 3.

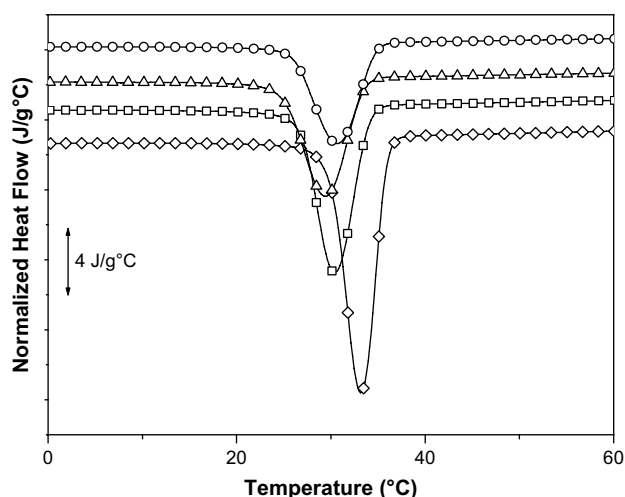


Fig. 3. Cooling thermograms for neat PCL and PCL/CHT semiIPNs. PCL ( $\diamond$ ), 10 wt.% ( $\square$ ), 20 wt.% ( $\triangle$ ) and 30 wt.% CHT ( $\circ$ ).

**Table 1**

Thermal properties of the semiIPNs. Crystallization enthalpy  $\Delta H_c$ , melting enthalpy  $\Delta H_f$ , melting temperature  $T_m$ , crystallization temperature  $T_c$  and crystallinity  $\chi_c$ .

PCL/CHT semiIPNs	$T_g$ (°C)	$\Delta H_c$ (J/g)	$\Delta H_f$ (J/g)	$T_m$ (°C)	$T_c$ (°C)	$\chi_c$ (%)
PCL	-61.5	57.8	65.4	57.0	32.5	46.9
10 wt.% CHT	-61.2	45.6	46.9	56.7	29.9	37.4
20 wt.% CHT	-58.5	37.9	41.0	56.4	28.8	36.8
30 wt.% CHT	-55.7	32.8	35.1	56.6	30.0	36.0

The main feature observed is the significant shift towards lower temperatures of the exothermal peak due to PCL crystallization in the semiIPNs with respect to pure PCL sample. The glass transition region broadens in the semiIPNs with respect to neat PCL (results not shown). The absolute values of glass transition temperature  $T_g$  (measured from second heating scan) and other characteristic parameters of the cooling and heating thermograms (crystallization point  $T_c$ , and melting point  $T_m$ , determined as the minimum of the exothermal peak measured on cooling and the maximum of the endothermic melting peaks respectively, crystallization enthalpy  $\Delta H_c$ , melting enthalpy  $\Delta H_f$ , both determined per gram of sample, and the degree of crystallinity  $\chi_c$ ) are listed in Table 1.

The fraction of PCL that crystallize in the semiIPNs was calculated as

$$\chi_c = \frac{\Delta H_f}{w_{PCL}\Delta H_f^0} \quad (3)$$

where,  $\Delta H_f$  is the melting enthalpy associated to the PCL peak in the DSC thermograms,  $\Delta H_f^0 = 139.5$  J/g represents the melting enthalpy of the single crystal [17] and  $w_{PCL}$  is the weight fraction of PCL in the semiIPN.

The temperature dependence of the storage modulus  $E'$ , and loss tangent for PCL/CHT semiIPNs (prepared without any PEO porogen) measured at a frequency of 1 Hz using DMA are represented in Fig. 4. Dynamic-mechanical analysis is a very sensitive technique for the study of the glass transition in complex systems. In this case, the main dynamic-mechanical relaxation of the amorphous PCL phase, associated to its glass transition, is clearly displayed as a broad peak around  $-40$  °C in the loss tangent, and a slight fall of the elastic modulus (Fig. 4).

The shift of the glass transition temperature (or the temperature of the loss tangent peak at the  $\alpha$  relaxation,  $T_{\alpha}$ ) with respect to those appearing in the pure component is a well accepted criterion for

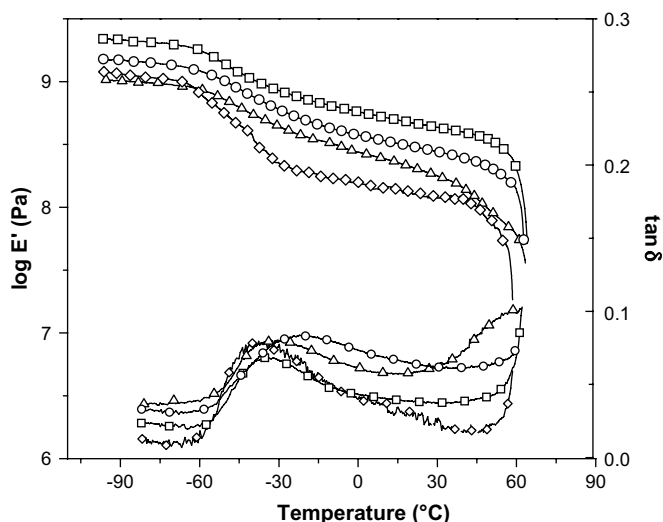


**Fig. 4.** Storage modulus and loss tangent for semiIPNs prepared without porogen and neat PCL. PCL ( $\diamond$ ), 10 wt.% ( $\square$ ), 20 wt.% ( $\triangle$ ) and 30 wt.% CHT ( $\circ$ ).

**Table 2**

Equilibrium swelling degree (Eq. (1) in the text) and porosity of the PCL/CHT scaffolds. The swelling degree was measured on samples prepared without any porogen (0 wt.% PEO).

PCL/CHT scaffolds	Swelling degree, w	Porosity (%)			
		0 wt.% PEO	30 wt.% PEO	45 wt.% PEO	55 wt.% PEO
10 wt.% CHT	0.22	21	34	51	58
20 wt.% CHT	0.37	33	32	54	61
30 wt.% CHT	0.58	25	37	60	64

miscibility and interphase interaction between the components of a polymer blend or composite. In our semiIPNs the main  $\alpha$  relaxation shifts towards higher temperatures: the maximum of the loss tangent peak shifted from  $-44$  °C in the sample with 10 wt.% to  $-30$  °C in the semiIPNs with 30 wt.% of CHT and the transition is very broad covering a temperature interval of 50 °C, and decreases its intensity as the CHT content in the sample increases. The elastic modulus measured at low temperatures, when the amorphous part of PCL is in the glassy state, is around 1 GPa, as expected for a semicrystalline polymer. At higher temperatures, the sudden drop of the elastic modulus at approx. 50 °C is due to the melting of PCL.

The basis of the procedure used to fabricate the scaffolds is the fact that PCL melting and recrystallization creates permanent links between the particles of the PCL/CHT semiIPNs. Even if no porogen is added, the air occupying the free space between the PCL/CHT particles originates certain porosity, between 20 and 30% (see Table 2). Consequently, an interpretation of the absolute values of the elastic modulus is difficult since it depends not only on the content of the stiff CHT component and its connectivity in the semiIPN but also on the porosity of the sample. Thus, the storage modulus of the sample containing 10 wt.% CHT is higher than those of the samples containing 20 or 30 wt.% when the contrary should be expected. Nevertheless as shown in Table 2 the porosity of the former is smaller than in scaffolds with higher CHT content.

The FTIR spectra of neat PCL, CHT and for all PCL/CHT semiIPNs are shown in Fig. 5. A characteristic band at  $3450$   $\text{cm}^{-1}$  is attributed to  $-\text{NH}_2$  and  $-\text{OH}$  groups stretching vibration and the band for amide I at  $1655$   $\text{cm}^{-1}$  is seen in the infrared spectrum of chitosan. Whereas the FTIR spectra of PCL show distinctive band centred at  $1725$   $\text{cm}^{-1}$  attributable to the carbonyl group stretching vibration in PCL structure. FTIR spectra of PCL/CHT semiIPNs exhibit noticeable changes compared with those of each neat component (Fig. 5A). The band of carbonyl group of PCL is shifted to higher wavenumbers (from  $1725$  in neat PCL to  $1748$   $\text{cm}^{-1}$ ) and a shoulder appeared at about  $1710$   $\text{cm}^{-1}$  as CHT content in the semiIPNs increases. The shoulder band is attributable to the hydrogen-bonded carbonyl groups with hydrogen-donating groups ( $-\text{OH}$  and  $-\text{NH}_2$ ) of chitosan (see Fig. 5B). Senda et al. [18,19] observed similar results in their studies of polycaprolactone/chitin and chitosan blends. In addition, the band at  $1640$   $\text{cm}^{-1}$  (attributed to  $\text{NH}_3^+$  formation) together with the band at  $1200$   $\text{cm}^{-1}$  (attributed to  $\text{P}=\text{O}$  groups of sodium tripolyphosphate used as crosslinked agent) more distinguishable in IR spectra of 30 wt.% CHT is indicative that semiIPNs are formed.

Fig. 6 shows the weight trace, TG, obtained in the TGA experiments for neat PCL, CHT and PCL/CHT semiIPNs at a heating rate of  $10$  °C/min in nitrogen atmosphere.

In addition Fig. 7 shows the derivative of the TGA trace for pure PCL and CHT and the 30 wt.% CHT semiIPN, the rest of curves have not been shown for the sake of clarity. PCL thermograms exhibit one stage of degradation from  $283$  to  $448$  °C with a maximum degradation temperature (from DTG) at  $386$  °C which is ascribed to chain scissions [20], called stage IV in Fig. 7. On the other hand, DTG curve of CHT displays three different stages, I, III and V. The first one

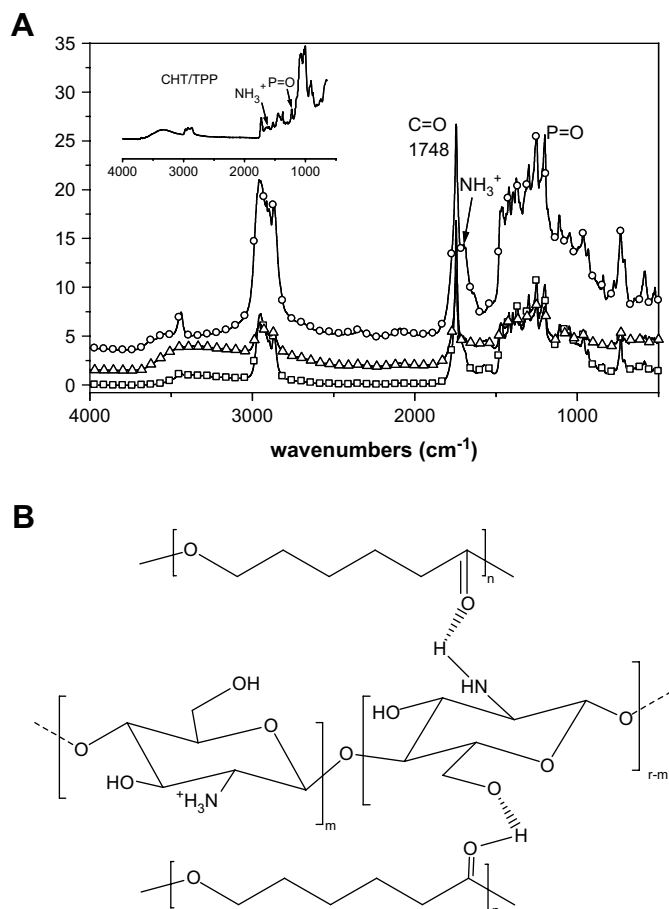


**Fig. 5.** SDR-FTIR spectra of PCL/CHT semiIPNs with different compositions, 10 wt.% (□), 20 wt.% (Δ) and 30 wt.% CHT (○) (A) and possible interaction between functional groups of PCL and CHT (B).

is located between 60 °C and 140 °C with a peak at 110 °C and is usually associated with a loss of water [21]. The second stage starts at 240 °C and reaches the maximum at 298 °C and the last weight lost stage has a peak at 550 °C. The two latter steps are attributed to a complex process including dehydration of the saccharide rings, depolymerisation and decomposition of the acetylated and deacetylated units of the polymer [22,23].

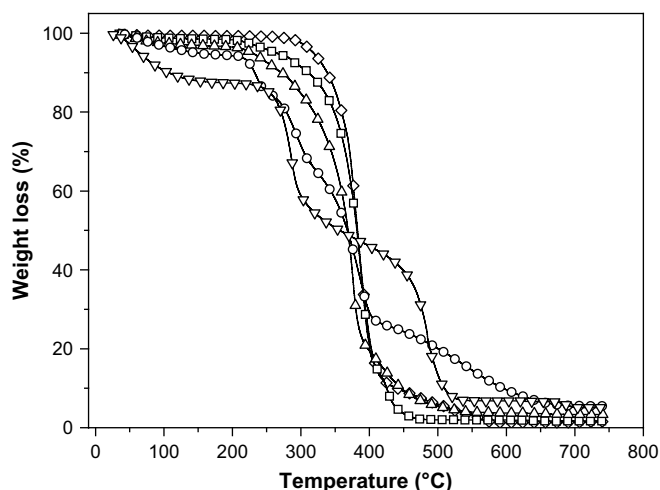


**Fig. 6.** TG thermograms obtained for neat chitosan, polycaprolactone and PCL/CHT semiIPNs. PCL (◇), 10 wt.% (□), 20 wt.% (Δ), 30 wt.% CHT (○) and CHT (▽).

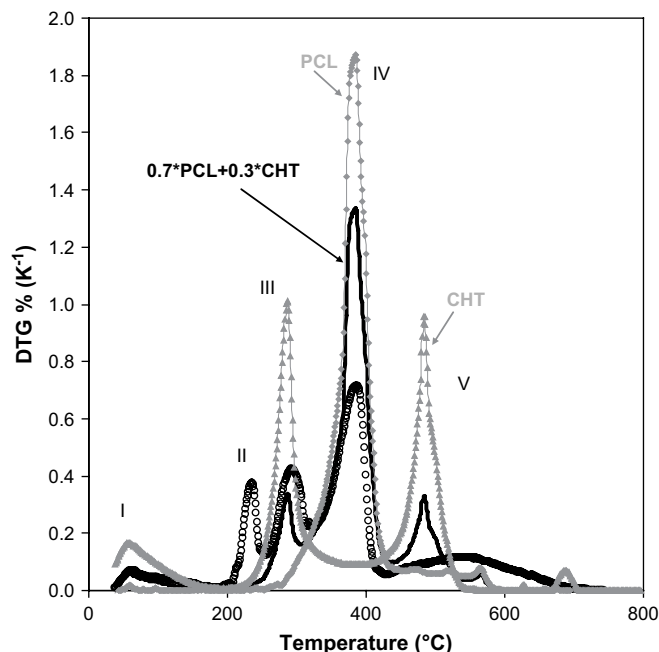


**Fig. 7.** DTG thermograms obtained for PCL (grey diamonds), CHT (grey triangles) and the semiIPN containing 30% CHT (open circles). The sum of the PCL and CHT thermograms multiplied by 0.7 and 0.3 respectively is also shown (solid black line).

The TG/DTG curves of PCL/CHT semiIPNs (Figs. 6 and 7) show the main features of the pure components but, there are two clear distinctive features: on the one hand a new peak appear in the DTG curve with a maximum around 220 °C in the sample containing 30 wt.% CHT (peak II in Fig. 7). In the same temperature interval a shoulder also appears in the other semiIPNs but it is not resolved as a peak (results not shown); on the other hand the high temperature CHT degradation extremely broadens as is clearly shown in TG and DTG peaks. The comparison of the experimental thermogram of 30 wt.% CHT chitosan semiIPN with the result of the sum of the thermograms of the pure components multiplied by their weight fraction in the semiIPN (black solid line in Fig. 6) shows that whereas peak I and III approximately agree with the corresponding weight loss of the CHT phase, peak IV is clearly less intense than what could correspond to PCL degradation. A quantification of the weight loss shows that the area under peak IV accounts only for around 60% of the PCL contained by the sample. Thus one may induce that the loss weight corresponding to stage II appearing in the semiIPNs corresponds to PCL chains that due to the interaction with CHT units degrades at lower temperatures than in pure PCL.

### 3.2. Morphological characterization

A sinterization process is used to fabricate the PCL/CHT scaffolds from semiIPNs. Even if no porogen is added, the air occupying the free space between the PCL/CHT particles originates certain porosity, between 20 and 30% (see Table 2). Interestingly enough, despite the reduced porosity, pores are well interconnected, as shown in Fig. 8A–C for samples containing 10, 20 or 30 wt.% CHT.

This porosity is too small for most of the tissue engineering applications, so scaffolds were prepared adding a certain amount of PEO microspheres as porogen. When the amount of PEO mixed with PCL/CHT particles was up to 55% by weight, the thermal treatment that melts both PEO and PCL and recrystallises them is able to join the PCL/CHT microparticles in such a way that the elimination of the porogen produces a consistent macroporous PCL/CHT scaffold, as shown in Fig. 8D–F (note the different magnification of these

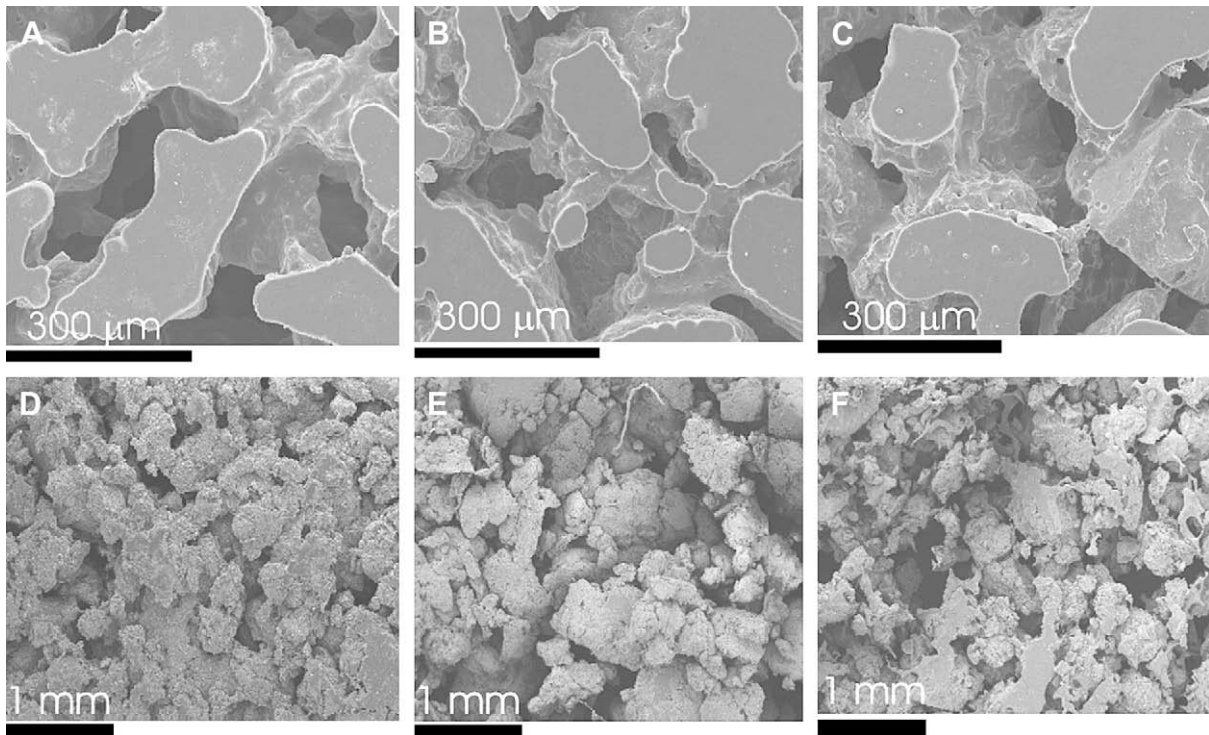


**Fig. 8.** SEM microphotographs of PCL/CHT scaffolds. (A, D) 10 wt.% CHT; (B, E) 20 wt.% CHT and (C, F) 30 wt.% CHT. A, B and C were prepared without any porogen. D, E and F after leaching out 55% of PEO particulates.

microphotographs with respect to those of the samples prepared without porogen). Still an open pore structure with well interconnected pores was obtained. The spherical shape of the PEO microparticles is lost in the melting and recrystallization processes and the shape of the pores is quite irregular. As listed in Table 2, the porosity of the scaffold continuously increases with the amount of porogen used in the fabrication process reaching values up to 60–65%, depending on the CHT content, when 55% by weight of PEO was used. Higher amounts of PEO yielded to scaffolds without mechanical integrity because when temperature is increased to 90 °C, the PCL/CHT particles remain dispersed in the PEO molten phase and do not adhere to each other during cooling.

The micromorphology of the PCL/CHT scaffolds (prepared without any porogen) can be observed in SEM pictures obtained at higher magnification (Fig. 9). The surface presents a characteristic microporosity and spherical CHT inclusions, around 1–2 μm, appear clearly at the surface of the macro-pores. This morphology was already found in PCL/CHT blends [9] obtained by precipitation from aqueous acetic acid co-solutions of PCL and CHT.

Dynamic swelling studies were performed in SBF for 6 days at 37 °C and the gain of weight was monitored as a function of time.

As can be expected, the swelling degree increases with the amount of hydrophilic – chitosan – component in the system (Table 2).

#### 4. Discussion

In a previous work PCL/CHT blends were prepared by casting from a solution [10]. It was proved that with that procedure a continuous CHT phase is obtained for CHT contents of the blend higher than 20 wt.%. In fact the sample containing 20 wt.% CHT maintained its geometrical integrity after extracting the polycaprolactone in chloroform. In this work, the procedure for blending chitosan and polycaprolactone is quite different. When the solution of CHT in aqueous 1 M acetic acid and that of PCL in glacial acetic acid are mixed transparent and apparently homogeneous solutions were obtained. After that, the polymer solutions were precipitated in an excess of sodium tripolyphosphate solution bath under strong agitation crosslinks chitosan favouring the entrapping of polycaprolactone chains in the chitosan network. The process yields a grounded material. Even if it is expected that a part of the PCL chains are interpenetrated with the chitosan network forming a semiIPN, the experimental results show that the system

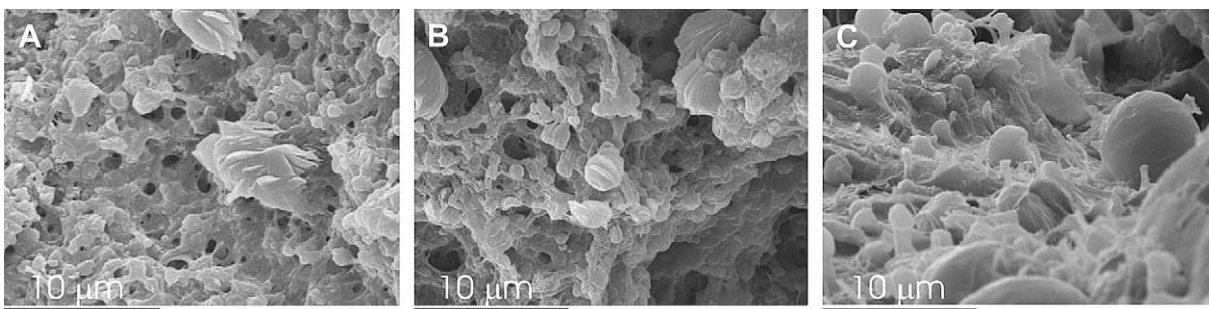


**Fig. 9.** SEM microphotographs of the microporosity in PCL/CHT scaffolds (prepared without any porogen). (A) 10 wt.% CHT; (B) 20 wt.% CHT and (C) 30 wt.% CHT.

is not completely homogeneous (as proved by the appearance of the glass transition of PCL and their ability to crystallize) and, mainly for low CHT contents a phase of pure semicrystalline PCL must coexist with the CHT phase.

After grounding the precipitate, a sheet with mechanical integrity can be produced just by melting and recrystallizing PCL. In this way the blend or semiIPN particles are joined in the contact points by the growth of new PCL crystals. The procedure gives as a result a porous material (Fig. 8) whose porosity ranges between 20 and 30% depending on the chitosan content. The elastic modulus of this material is quite high at low temperatures, when the amorphous part of PCL is in the glassy state, between 1 and 3 GPa (Fig. 4) depending on the CHT content and on the porosity of the sample. These high values prove that the semiIPN particles are well adhered to each other forming a continuous material. The modulus drops around  $-50\text{ }^{\circ}\text{C}$  when the glass transition of PCL takes place, but it reaches higher values than neat PCL showing the reinforcing effect of the chitosan network. Of course, when PCL melts, around  $60\text{ }^{\circ}\text{C}$ , the sample flows because the joining points between the semiIPN particles are lost.

It is interesting to note that the crystallinity of PCL in the samples (crystallized from the melt) is significantly smaller than in pure PCL. This means that a part (around 20% according to the data of Table 1) of the PCL chains is not able to participate in the crystalline structure probably because they are dispersed inside the chitosan network. This behaviour is in agreement with the results obtained by Honma et al. [18], that was attributed to the hydrogen bond interactions between functional groups present in CHT structure ( $-\text{NH}_2$  and OH) and carbonyl groups present in PCL. Such interactions occur in the amorphous phase, so the crystallization of PCL is suppressed. The displacement of some absorption IR peaks in the blends with respect to the pure PCL or CHT also proves that a significant part of the polymer chains of both components is mixed at distances in the order of magnitude of the molecular sizes. The shift of the high temperature TGA peak of chitosan (stage IV of the degradation) towards higher temperatures and its change of shape in the semiIPNs with respect to the pure CHT, as well as the degradation of part of the PCL chains at much lower temperatures than in pure PCL also support this conclusion. Another interesting feature is that the crystallization DSC peak (Fig. 3) is shifted in the blends towards lower temperatures with respect to pure PCL. This means that the surfaces of chitosan domains do not act as nucleation points for PCL crystallization as it was found in the blends obtained by casting from the solution in Ref. [9].

The pore structure of these samples, shown in the SEM microphotographs of Fig. 8, seems to be adequate for cell ingrowth, with interconnected pores with sizes in the order of  $100\text{ }\mu\text{m}$ . Nevertheless, porosity in between 20 and 30% is clearly insufficient for tissue engineering applications. Macroporous scaffolds can be obtained with these materials by adding a porogen during the sintering of the PCL/chitosan particles. Poly(ethylene oxide), PEO, particles have been used to do that in this work. The melting point of PEO is very close to that of PCL. PCL/chitosan particles were dry mixed with PEO particles and heated to  $90\text{ }^{\circ}\text{C}$  to melt both PCL and PEO. When the sample is cooled again, recrystallization of both materials produces co-continuous phases: one of them consisting of the sintered PCL/chitosan semiIPN and the other one of PEO. Then PEO phase was dissolved in water leaving an additional volume fraction of interconnected pores in agreement with the fraction of PEO added previously. Table 2 shows the dependence of the porosity of the scaffolds on the weight fraction of porogen added during the sintering process.

The dynamic-mechanical properties of the scaffolds (prepared without any porogen) reflect the influence of both composition and porosity of the system. Even if higher values of the modulus are

expected as the fraction of CHT in the sample increases, the different porosities obtained in the preparation process (Table 2) lead to higher modulus for the sample 10 wt.% CHT (Fig. 4). The shift of the main,  $\alpha$  relaxation of PCL towards higher temperatures with increasing amounts of CHT is another feature showing the interaction between the two phases which suggests that the conformational motions of the amorphous PCL chains are affected by the nearby CHT chains. Above  $50\text{ }^{\circ}\text{C}$ , melting of PCL starts and the elastic modulus falls steeply. Since the scaffold is prepared starting with semiIPN microparticles which are sintered by thermal treatments which include melting and recrystallization of the PCL phase, the mechanical integrity of the scaffold is only assured by the continuity of the PCL phase which disappears when it melts.

## 5. Conclusions

Apparently homogeneous co-solutions were obtained mixing PCL solution in 1 M acetic acid with chitosan solutions in pure acetic acid for CHT/PCL weight ratios up to 30/70. Then, a poly( $\epsilon$ -caprolactone)/chitosan semiIPN was successfully prepared by simultaneous precipitation and chitosan crosslinking with tripolyphosphate. High porosity semiIPN scaffolds with good mechanical properties were prepared. Phase separation takes place in the semiIPN but the displacement of some IR absorption peaks in the blends (in comparison to those of pure components), the lower value of PCL crystalline fraction in the semiIPNs, the change in the temperature of the main dynamic-mechanical relaxation with increase in chitosan content and the shift in the TGA peaks with respect to the pure components might point towards the fact that, there might be an interaction between PCL and CHT chains situated at distances in the order of molecular dimensions.

## Acknowledgements

The support from the Spanish Ministry of Science through the MAT2006-08120 project (including the FEDER financial support) is kindly acknowledged. Support from FCT, through projects POCTI/FIS/61621/2004 and PTDC/FIS/68517/2006. D. García Cruz thanks the PhD fellowship from Generalitat Valenciana (CTBPRB/2005/078).

## References

- [1] Venugopal J, Zhang YZ, Ramakrishna S. *Nanotechnology* 2005;16:2138.
- [2] Van Lieshout MI, Peters GWM, Rutten MCM, Baaijens FPT. *Tissue Eng* 2006;12:481.
- [3] Gross RA, Kalra B. *Science* 2002;297:803.
- [4] Hollister SJ. *Nat Mat* 2005;4:518.
- [5] Kiersnowski A, Piglowski J. *Eur Polym J* 2004;40:1199.
- [6] Escobar Ivirico JL, Costa Martínez E, Salmerón Sánchez M, Muñoz Criado I, Gómez Ribelles JL, Monleón Pradas M. *J Biomed Mater Res B* 2007;83:266.
- [7] Singh RP, Pandey JK, Rutot D, Degee P, Dubois P. *Carbohydr Res* 2003;338:1759.
- [8] Vázquez-Torres H, Cruz-Ramos CA. *J Appl Polym Sci* 2003;54:1141.
- [9] Sarasam AR, Madhally SV. *Biomaterials* 2005;26:5500.
- [10] García Cruz DM, Gómez Ribelles JL, Salmerón Sánchez M. *J Biomed Mater Res B* 2008;85:303.
- [11] Yang A, Wu R Zhu P. *J Appl Polym Sci* 2001;81:3117.
- [12] Cho YW, Han SS, Ko SW. *Polymer* 2000;41:2033.
- [13] Madhally SV, Matthew HWT. *Biomaterials* 1999;20:1133.
- [14] Sarasam AR, Samli AI, Hess L, Ilnat MA, Madhally SV. *Macromol Biosci* 2007;7:1160.
- [15] Klemperer D, Sperling JH. *Interpenetrating polymer networks*. In: *Advances in chemistry series*, vol. 239. Washington: American Chemical Society; 1994.
- [16] Takadama H, Kokubo T. *Biomaterials* 2006;27:2907.
- [17] Crescenzi V, Manzini G, Calzolari G, Borri C. *Eur Polym J* 1972;8:449.
- [18] Honma T, Senda T, Inoue Y. *Polym Int* 2003;52:1839.
- [19] Senda T, He Y, Inoue Y. *Polym Int* 2001;51:33.
- [20] Sivalingam G, Karthik V, Madras G. *J Anal Appl Pyrolysis* 2003;70:631.
- [21] Peniche V, Argüelles-Monal W, Davidenko N, Sastre R, Gallardo A, San Román J. *Biomaterials* 1999;20:1869.
- [22] Peniche C, Argüelles-Monal V, San Román J. *Polym Degrad Stab* 1993;39:21.
- [23] García I, Peniche C, Nieto JM. *J Therm Anal* 1983;21:189.